JPET Fast Forward. Published on March 25, 2009 as DOI: 10.1124/jpet.108.146175

Title Page

Compartmentalized β Subunit Distribution Determines Characteristics and Ethanol Sensitivity of Somatic, Dendritic, and Terminal BK Channels in the Rat CNS

Wynne PM, Puig SI, Martin GE, Treistman SN

Brudnick Neuropsychiatric Research Institute

University of Massachusetts Medical School

Worcester, Massachusetts 01605

(PM, SP, GE, SN)

Running Title Page

Running Title: Beta subunit determines regional characteristics of BK

Corresponding Author: Steven N. Treistman, Ph.D.

Institute of Neurobiology

201 Blvd del Valle, San Juan, Puerto Rico 00901,

University of Puerto Rico, PR

Phone: 787 721 4149

Fax: 787-721-4584

Steven.Treistman@upr.edu

36 Text Pages

0 Tables

6 Figures

40 Refs

250 Words in Abstract

639 Words in Introduction

1406 Words in Discussion

Section Assignment: Cellular and Molecular

List of non-standard abbreviations; dendritic localizer sequence (DLS), hypothalamic-neurohypophysial system (HNS), iberiotoxin (IbTX), large conductance calcium activated potassium (BK) channels, magnocellular neurons (MCNs), oxytocin (OXT), stress-regulated exon (STREX), supraoptic nucleus (SON), vasopressin (AVP).

JPET Fast Forward. Published on March 25, 2009 as DOI: 10.1124/jpet.108.146175
This article has not been copyedited and formatted. The final version may differ from this version.

Abstract

Neurons are highly differentiated and polarized cells, whose various functions depend upon the compartmentalization of ion channels. The rat hypothalamic-neurohypophysial system (HNS), in which cell bodies and dendrites reside in the hypothalamus, physically separated from their nerve terminals in the neurohypophysis, provides a particularly powerful preparation in which to study the distribution and regional properties of ion channel proteins. Using electrophysiological and immunohistochemical techniques we characterize the BK channel in each of the three primary compartments (soma, dendrite, and terminal) of HNS neurons. We find that dendritic BK channels, in common with somatic channels, but in contrast to nerve terminal channels, are insensitive to iberiotoxin. Furthermore, analysis of dendritic BK channel gating kinetics indicates that they, like somatic channels, have fast activation kinetics, in contrast to the slow gating of terminal channels. Dendritic and somatic channels are also more sensitive to calcium and have a greater conductance than terminal channels. Finally, while terminal BK channels are highly potentiated by ethanol, somatic and dendritic channels are insensitive to the drug. The biophysical and pharmacological properties of somatic and dendritic vs. nerve terminal channels are consistent with the characteristics of exogenously expressed αβ1 vs. αβ4 channels, respectively. Therefore, one possible explanation for our findings is a selective distribution of auxiliary β1 subunits to the somatic and dendritic compartments and β4 to the terminal compartment. This hypothesis is supported immunohistochemically by the appearance of distinct punctuate β1 or β4 channel clusters in the membrane of somatic and dendritic or nerve terminal compartments, respectively.

Introduction

Ion channel compartmentalization between specific brain regions and various neuronal populations has been known for many years. Recently, technological advances have permitted researchers to probe the distribution of channel subtypes on a subcellular level. Here we have utilized a unique system, the hypothalamic-neurohypophysial system (HNS), which allows us to examine dendrites, cell bodies, and individual nerve terminals within the same population of magnocellular neurons (MCNs). The HNS is an ideal model system to study compartmentalization of channel properties because the three neuronal domains (dendrite, cell body, and nerve terminal) can be easily distinguished from one another. The large (20-30 μm) magnocellular neurons of the supraoptic nucleus (SON) send axonal projections to the posterior pituitary (neurohypophysis) where they terminate in thousands of nerve endings which release oxytocin (OXT) or vasopressin (AVP) into systemic circulation. MCN dendrites, on the other hand, project toward the ventral surface of the brain forming a dense interlaced network that releases OXT or AVP centrally. Morphologically, HNS axons have few if any collaterals, allowing them to be easily distinguished from dendrites.

Large conductance calcium activated potassium (BK) channels play a prominent role in cellular excitability from repolarizing neuronal action potentials to modulating contractility in vasculature. They are found ubiquitously throughout the brain and are highly conserved in mammals. BK channels are activated by both cell membrane depolarization and increases in intracellular calcium, allowing them to function as coincidence detectors that integrate intracellular calcium levels and membrane voltage. BK channels may be homomeric or heteromeric and are

JPET Fast Forward. Published on March 25, 2009 as DOI: 10.1124/jpet.108.146175
This article has not been copyedited and formatted. The final version may differ from this version.

composed of four seven-transmembrane α subunits which form the selectivity pore of the channel.

Currently, four β subunits (β1- β4) have been cloned and characterized. Association of the α subunit with various β subunits modulates channel properties, including kinetic behavior, voltage dependence, calcium sensitivity, and pharmacological attributes such as sensitivity to the channel blockers, iberiotoxin and charybdotoxin (Dworetzky et al., 1996; Lippiat et al., 2003). To date, studies examining the regional distribution of BK β subunits indicate that they are relatively tissue specific. Several studies indicate that β1 subunits are localized primarily in smooth muscle, showing less expression in the brain (Jiang et al., 1999). β2 subunit expression is especially abundant in ovaries, while β3 shows the highest expression in the pancreas and testis. The β2 and β3 subunits are only weakly detected in other tissues, including brain (Wallner et al., 1996; Brenner et al., 2000). In contrast to the other β subunits, β4 is highly expressed in brain, and only weakly detected in other tissues (Brenner et al., 2000).

On the subcellular level, few studies have attempted to describe BK channel distribution, characterization, and subunit composition in all three compartments of a neuron. Studies have described the immunolocalization of BK channels in the dendrites and nerve terminals of hippocampal pyramidal neurons, but did not biophysically characterize or identify the subunit composition of the channels (Sailer et al., 2006). In another example, Benhassine and Berger determined that the biophysical properties of dendritic and somatic BK channels in layer 5 pyramidal neurons of the somatosensory cortex were identical, but did not examine channels in nerve terminals (Benhassine and Berger, 2005). We have previously reported that dendritic and

somatic BK channels in rat nucleus accumbens neurons display different biophysical properties, which could be explained by a predominance of BK β1subunits in the dendritic compartment and BK β4 subunits in the cell body (Martin et al., 2004). Again, due to limitations of the preparation, this study was unable to examine BK channels in nucleus accumbens nerve terminals. Here, we focus on BK channels within HNS magnocellular neurons, and describe the characteristics of BK channels in each of the three major compartments of a CNS neuron. These findings may have functional significance in understanding how peptide release from the dendritic, somatic and nerve terminal compartment are differentially regulated (reviewed in Ludwig and Leng, 2006).

JPET Fast Forward. Published on March 25, 2009 as DOI: 10.1124/jpet.108.146175
This article has not been copyedited and formatted. The final version may differ from this version.

Methods

Isolated SON Cell Bodies

Adult Sprague Dawley rats (150-250 g) were decapitated, the brain removed and placed into a dish containing oxygenated ice-cold (4ºC) high sucrose cutting solution. 500 µm slices were obtained using a Vibroslicer, the SON isolated with the aid of a dissecting microscope, and transferred to an oxygenated (100% O_2 with constant stirring) HBSS solution containing Protease XIV from *Streptomyces griseus* (Sigma-Aldrich, St. Louis, MO) for 15 minutes. The SON disks were then transferred to EBSS (holding) solution oxygenated with 95%O_2/5%CO_2 for 45 minutes. The tissue was then mechanically triturated in sodium isethionate solution using fire polished Pasteur pipettes with successively smaller tip diameters. Dissociated cell bodies were then transferred to a 35 mm Petri dish placed on the stage of an inverted microscope (Nikon Diaphot). The cells were allowed to settle for 15 min before perfusing with 60 ml regular Locke's solution at a rate of 4 ml/min. Electrophysiological recordings were subsequently obtained from either the cell body or dendrite. In contrast to axons, which have a uniform width and lack any branches, dendrites were identified morphologically by their tapered appearance and branching (Figure 1A).

Isolated Neurohypophysial Terminals

The neurohypophysis was removed from the animal within 1 min of sacrifice and placed in low-calcium Locke's solution. To expose the neurohypophysis, the pars intermedia was dissected away and discarded. Terminals were homogenized in a solution containing in mM: 270 sucrose, 10 HEPES, and 1 mM EGTA, pH 7.3, and transferred to a 35 mM dish where they were allowed

to settle. The terminals were then processed for immunohistochemistry or electrophysiology. For electrophysiological measurements, dissociated terminals were identified by their spherical shape, approximately 6 um diameter, lack of nuclei, and golden color under Hoffman phase-contrast optics. Prior to ethanol challenge, the terminals were first bathed in low-calcium (3 µM free-Ca^{2+}) Locke's solution followed by regular Locke's solution.

Single Channel Recordings

Recording electrodes were pulled (Sutter Instruments, Novato, CA) and fire-polished from borosilicate capillary glass (Drummond, Bromall, PA) to a final resistance of 4-8 MΩ. Currents were recorded in voltage-clamp mode with a HEKA EPC 10 amplifier at a sampling rate of 10 kHz and low-pass filtered at 2.0 kHz with an eight-pole Bessel filter. Potentials and currents were digitized, curve-fit, measured, stored, and plotted using Patchmaster acquisition and analysis software (HEKA Elektronik, Lambrecht/Pfalz, Germany).

Data analysis

NP_o values were calculated from all-points amplitude histograms by fitting the histogram with a sum of Gaussian functions using a Levenberg–Marquardt algorithm. NP_o data as a function of voltage were fitted with a Boltzmann function of the type: $P_o = (1 + \exp - K(V - V_{0.5}))^{-1}$, where K is the logarithmic potential sensitivity and $V_{0.5}$ the potential at which P_o is half-maximal. When the NP_o–voltage relationship is fitted by a Boltzmann curve, a plot of $\ln NP_o$ versus voltage is linear at low values of P_o. In this plot, the reciprocal of the slope is the potential needed to produce an *e*-fold change in NP_o, which is routinely used to measure the voltage dependence of BK channel gating. The unitary conductance (γ) was taken as the slope of the unitary current amplitude–voltage relationship. Values for unitary current were obtained from the Gaussian fit of all-points

JPET Fast Forward. Published on March 25, 2009 as DOI: 10.1124/jpet.108.146175
This article has not been copyedited and formatted. The final version may differ from this version.

amplitude histograms by measuring the distance between the modes corresponding to the closed state and the first opening level. In single-channel patches, durations of open and closed times were measured with half-amplitude threshold analysis. A maximum-likelihood minimization routine was used to fit curves to the distribution of open or closed times. For all experiments, voltages given correspond to the potential at the intracellular side of the membrane.

Macroscopic currents were compiled by summing 100 consecutive single channel traces obtained by stepping the membrane of an inside-out patch from a holding potential of 0 mV to + 40 mV, in the presence of 10 µM free-Ca^{2+}. Leak currents were subtracted on-line. To yield the macroscopic current, traces were summed and the activation kinetics subsequently fit using Fitmaster software (HEKA Elektronik, Lambrecht/Pfalz, Germany).

Ethanol and Iberiotoxin Application

Recording electrode tips were positioned in the 'mouth' of the perfusion pipe (hematocrit tubes) to prevent contamination from solutions potentially leaking from nearby tubes. Three 20 sec control traces in the presence of 5 µM-free Ca^{2+} solution were taken to determine baseline channel activity. Ethanol or iberiotoxin were applied to inside-out or outside-out patches, respectively.

Experimental Solutions

High potassium pipette solution contained the following in mM: 135 K-Gluconate, 1 $MgCl_2$, 2.2 $CaCl_2$, 15 HEPES, 4 EGTA, and 4 HEDTA. Regular Locke's solution contained the following in mM: 2 KCl, 142 NaCl, 2 $MgCl_2$, 2 $CaCl_2$, 13 glucose, and 15 HEPES. During all recording sessions, excised patches were exposed to (in mM): 135-140 K-gluconate, 0-4 HEDTA, 0-4

EGTA, 15 HEPES, 1 $MgCl_2$, and 0.5-2.2 $CaCl_2$. HEDTA, EGTA, and $CaCl_2$ concentrations were adjusted to obtain the desired concentrations of free calcium, ranging from 1 to 25 µM. Free-Ca^{2+} concentrations were determined by the Max Chelator Sliders software (C. Patton, Stanford University) and confirmed with a Kwik-Tip calcium probe (World Precision Instruments, Sarasota, FL). In these conditions, K+ concentrations on either side of membrane patches were the same in all experiments. Regular Locke's solution was used to wash the recording chamber only.

Immunohistochemistry

To stain the SON, a block of brain tissue was fixed in 4% paraformaldehyde (PFA). After immersion in 20% sucrose, tissue was embedded in 6% gelatin-egg yolk mixture and exposed to concentrated formaldehyde vapors for at least 3 days (4ºC). After hardening, 50 µM coronal sections were cut on a freezing microtome, placed in 1X PBS, and transferred to wells. HNS terminals were dissociated, as described previously, allowed to settle for 15 min on glass bottom culture dishes (MatTek, Ashland, MA), and fixed in 4% PFA. Both the terminals and SON tissues slices were then permeabilized and blocked in a solution containing 10% NGS, 0.1% BSA, 0.4% Triton-X 100 in PBS/0.02% sodium azide, pH 7.4, for 1 hr at room temperature.

Permeabilized SON sections were incubated with primary antibodies to polyclonal anti-BK β1 (1:100; Alomone, Jerusalem, Israel) or polyclonal anti-BK β4 subunit (1:100; Alomone, Jerusalem, Israel) overnight at 4˚C. After incubation, SON slices were rinsed and incubated for 1 hr at room temperature with Alexa 488-tagged anti-rabbit secondary antibody (1:300; Molecular Probes, Eugene, OR) for 1 hr at room temperature. After rinsing, SON sections were

JPET Fast Forward. Published on March 25, 2009 as DOI: 10.1124/jpet.108.146175
This article has not been copyedited and formatted. The final version may differ from this version.

incubated with goat anti-vasopressin (1:100, Santa Cruz Biotechnology, Santa Cruz, CA) for 2 hours at room temperature, rinsed, and incubated with Alexa 594-tagged anti-goat secondary antibody. After ample washing with PBS, SON tissue slices were mounted on microslides (SuperFrost Plus; VWR Scientific, West Chester, PA) using Prolong Antifade medium (Invitrogen, Carlsbad, CA).

Permeabilized nerve terminals were incubated with primary antibodies to polyclonal anti-BK β1 (1:100; Alomone, Jerusalem, Israel) or polyclonal anti-BK β4 subunit (1:100; Alomone, Jerusalem, Israel) overnight at 4˚C. After incubation, terminals were rinsed and incubated for 1 hr at room temperature with Alexa 594-tagged anti-rabbit secondary antibody (1:300; Molecular Probes, Eugene, OR) for 1 hr at room temperature. After rinsing, terminals were incubated with goat anti-vasopressin (1:100, Santa Cruz Biotechnology, Santa Cruz, CA) for 2 hours at room temperature, rinsed, and incubated with Alexa 350-tagged anti-goat secondary antibody. After after rinsing, terminals were incubated with mouse anti-oxytocin (1:100, a gift from Dr. H. Gainer) for 2 hours at room temperature, rinsed, and incubated with Alexa 488-tagged anti-mouse secondary antibody for 1 hour at room temperature. Coverslips were placed in glass bottom culture dishes using Prolong Antifade medium (Invitrogen, Carlsbad, CA). Control experiments were performed to insure the specificity of primary antibodies (anti-β1 and anti-β4) by adding commercially available blocking peptide which completely ablated staining. A Zeiss Axiovert inverted microscope and Axiovision 4.5 software package (Carl Zeiss, Inc., Thornwood, NY) were used to acquire and deconvolve Z-stacks of fluorescent images, and perform subsequent analysis.

To measure the intensity of specific BK β1 and β4 staining in each cell compartment a deconvolution fast iterative algorithm was applied to sharpen the signal; the resulting images were used for quantification; each compartment of the cell (soma, dendrite, terminal) was outlined and the average fluorescent density for each channel color was measured within these outlines; mean density values were obtained from the corresponding histograms generated in Photoshop (Adobe Systems, San Jose, CA). (The boundaries of each region were determined using the DIC image of the terminal overlapped onto the channel expression image).

Statistics

Unless otherwise indicated, statistical significance between various groups was analyzed using Student's t test (Statistica, version 5.5; StarSoft, Tulsa, OK). All data are expressed as average ± SEM, and $p < 0.05$ were considered to be statistically significant.

JPET Fast Forward. Published on March 25, 2009 as DOI: 10.1124/jpet.108.146175
This article has not been copyedited and formatted. The final version may differ from this version.

Results

SON dendrites express functional BK channels

Previous studies reported the presence of BK channels in SON cell bodies and their nerve terminals in the neurohypophysis (Wang et al., 1992; Dopico et al., 1999). In order to extend the characterization of BK channels to include the dendritic compartment, we first confirmed that BK channels are present in the dendrite. Figure 1A shows a micrograph of a micropipette placed on a dendrite. We assessed basic electrophysiological properties including voltage sensitivity, calcium sensitivity, and conductance of dendritic channels in inside-out patches. Dendritic single channel currents were elicited by depolarizing the membrane from -80 mV to +80 mV in 20 mV increments while perfusing the intracellular surface with 5 μM free-Ca^{2+}. For the channels shown in Fig. 1B, their open probability was very low at potentials below -40 mV, and did not increase further above +40 mV. As such, they did not provide further useful information and are not shown. Thus, the activity of a two-channel patch recorded between -40 mV and +40 mV is shown in Figure 1B. At -40 mV, the channel displays a low open probability (NPo = 0.097) but as the channel membrane is depolarized to +40 mV the channels spend more time in the open state (NPo = 0.92). The same patch was then clamped at -40 mV and the cystolic face exposed to 1, 5, and 10 μm free-Ca^{2+}. The channels are extremely calcium dependent, exhibiting low activity in 1 μm free-Ca^{2+} (NPo = 0.001), increasing activity to an NPo of 0.169 in the presence of 5 μm free-Ca^{2+}, and reaching a nearly persistent open state in 10 μm free-Ca^{2+} (NPo = 0.79) (Figure 1C). Figure 1D shows a plot of the current amplitude *vs*. the membrane potential of a dendritic channel. The current-voltage relationship was well-fitted with a linear regression (r = 0.99) yielding a slope conductance of 261 pS. In addition, current reversed at 0 mV in symmetric potassium conditions, $[K]_i = [K]_o$, indicating the channel is selective for potassium. These data

JPET Fast Forward. Published on March 25, 2009 as DOI: 10.1124/jpet.108.146175
This article has not been copyedited and formatted. The final version may differ from this version.

are consistent with the known features of BK channels including potassium selectivity, large conductance (>180 pS), and sensitivity to intracellular calcium (McManus, 1991).

In order to dependably compare the properties of BK channels in each of the three compartments, we repeated previously published characterizations of several BK channel parameters in the HNS cell body and nerve terminal in addition to those performed in the dendrite.

Conductance

In symmetric 135 mM K^+, with the intracellular face of inside-out patches exposed to 5 µM free-Ca^{2+}, the conductance of dendritic BK channels was 247.0 ± 11.2 pS, n = 7. In contrast, under identical conditions BK channels in nerve terminals had a conductance of 219 ± 4.84 pS, n = 4 (Figure 2A) consistent with previously reported values (Pietrzykowski et al., 2004). Values obtained for cell body channels, 250.7 ± 9.4 pS (n = 9) in 5 µM free-Ca^{2+} were very similar to dendritic channels. When exposed to 10 µM free-Ca^{2+} the conductance of somatic and dendritic channels was again similar, 248.3 ± 14.5 pS (n = 8) and 254 ± 7.03 pS (n = 6), respectively (Figure 2A). The conductance of BK channels from terminals in presence of 10 µM free-Ca^{2+} was obtained from a previous publication (Dopico et al., 1996).

Calcium Dependence

Figure 2B shows the normalized NPo of BK channels from SON terminals, soma, and dendrites as a function of membrane potential. The graph shows that the open probability of BK channels is steeply voltage dependent. The NPo-voltage relationship could be well-fitted with a Boltzmann

JPET Fast Forward. Published on March 25, 2009 as DOI: 10.1124/jpet.108.146175
This article has not been copyedited and formatted. The final version may differ from this version.

equation. Consistent with previous data (Dopico et al., 1999), nerve terminal BK channels were less sensitive to 10 µM free-Ca^{2+} than somatic channels ($V_{0.5}$ was -8.9 ± 3.5 mV, n = 7 in terminals and -30.6 ± 3.7 mV, n = 7 in cell body). Dendritic BK channels showed sensitivity to 10 µM free-Ca^{2+} similar to somatic channels ($V_{0.5}$ was -22.5 ± 4.2 mV, n = 9) (Figure 2B). In addition, the voltage necessary to produce an *e*-fold change in open probability (see Methods; reciprocal of the slope of the ln(Po)-V relationship at low Po) was similar for both somatic and dendritic SON channels (10.7 ± 1.5 and 11.6 ± 1.4, respectively). In the terminals, however, the voltage necessary to produce an *e*-fold change in open probability was 24 ± 2.8 mV. Taken together, these data suggest a relatively homogeneous BK channel profile in the somatic and dendritic compartments, which is markedly different from the channel population in the nerve terminal.

Because of the heavy dependence of BK channel open probability on calcium concentration we determined whether the similarity between dendritic and somatic BK channels open probability extended across a range of calcium concentrations. As shown in Figure 2C, the open probability of BK channels is steeply calcium and voltage dependent, as the calcium concentration is decreased the membrane must be depolarized more to produce a similar open probability (seen as a shift to the right). The graph shows the similarity between cell body and dendritic channels obtained from an examination of channel activity in 5, 10, and 25 µM free-Ca^{2+}. The potential at which half of the BK channels were open ($V_{0.5}$) in 25 µM free-Ca^{2+} was -65.6 ± 2.9 mV (n = 12) and -68.7 ± 3.3 mV (n = 10) in the soma and dendrites, respectively. In 10 µM free-Ca^{2+} $V_{0.5}$ was -30.6 ± 3.7 mV (n = 7) and -22.5 ± 4.2 mV (n = 9) in the soma and dendrites, respectively. Finally, in 5 µM free-Ca^{2+} $V_{0.5}$ was 8.5 ± 3.7 mV (n = 8) and 13.1 ± 1.9 mV (n = 11) in the soma

JPET Fast Forward. Published on March 25, 2009 as DOI: 10.1124/jpet.108.146175
This article has not been copyedited and formatted. The final version may differ from this version.

and dendrites, respectively (Figure 2C). In summary, we found that the NPo-voltage relationship of dendritic and somatic channels is indeed very similar across a range of calcium concentrations.

Activation kinetics of BK channels in cell bodies and dendrites vs. nerve terminal compartments.

Although whole-cell patch clamp is generally used to study kinetic properties such as activation, we could not use this approach, because it would not have enabled us to independently examine BK channel properties in each region of the cell. Moreover, single channel records assure that our data is not contaminated with non-BK currents. Therefore, to study channel kinetics we compiled a cumulative current trace from the summation of 100 repetitively evoked single channel sweeps. The resulting current trace resembles the classical macroscopic current recorded in whole-cell patch clamp configuration. The membrane of an inside-out patch was stepped from a holding potential of 0 mV to + 40 mV in the presence of 10 µM free-Ca^{2+}. A typical example showing 7 of 100 consecutive traces from somatic, dendritic, and nerve terminal channels is shown in Figures 3A-C. An example of the compiled macroscopic current from the soma, dendrite, and nerve terminal is shown in Figures 3D-F. In both the cell body and dendrite, currents were well fitted with a single exponential, τ was 3.4 ± 1.18 ms (n = 6) in the soma and 5.7 ± 2.34 ms (n = 7) in the dendrites, indicating these channels have relatively fast activation kinetics. In contrast, nerve terminal channels display much slower gating kinetics, τ = 22.7 ± 4.19 ms, n = 3.

Ethanol selectively potentiates nerve terminal but not somatic and dendritic BK channels.

JPET Fast Forward. Published on March 25, 2009 as DOI: 10.1124/jpet.108.146175
This article has not been copyedited and formatted. The final version may differ from this version.

The BK channel is a well-studied target of ethanol action, and while BK channels in HNS terminals are highly sensitive to ethanol, exhibiting increased channel activity within a few minutes, BK channels in the cell body of these neurons are insensitive to the drug (Dopico et al., 1999). Here, we examine the sensitivity of dendritic BK channels (Fig. 4). The ethanol sensitivity of BK channels in proximal dendrites (20-40 µM from the soma) was examined in inside-out patches in the presence of 5 µm free-Ca^{2+} at a membrane potential of -40 mV. The ethanol concentrations chosen were within a clinically relevant range from 20 mM EtOH (resulting in intoxication) to 100 mM EtOH (lethal in naïve subjects) (Madeira et al., 1993; Ruela et al., 1994). In the dendrite, the baseline probability of BK channel opening is low (nPo = 0.142) at -40 mV. During application of 50 mM EtOH, channel activity was recorded every 60 seconds for 10 minutes. Throughout the entire period of EtOH exposure channel activity remained unchanged (99 ± 14 % of control; n = 4) (Figure 4A/D). Similar results were obtained with 25 and 100 mM ethanol (99 ± 19 % of control values, n = 4, and 107 ± 29 % of control, n = 4, respectively) (Figure 4D). Neither 25, 50 nor 100 mM EtOH potentiated somatic channels (102 ± 17 % (n = 3), 111 ± 16 % of control (n = 3), and 118 ± 21 % respectively) (Figure 4B/D) further supporting the notion that cell body and dendrite channels are similar. In contrast, EtOH greatly potentiated the activity of channels in dissociated nerve terminals in a dose-dependent fashion. The peak effect was observed with 50 mM EtOH (673 ± 171%, n = 3), consistent with previous data (Dopico et al.,1996; Pietrzykowski et al., 2004) (Figure 4C/D). The response of BK channels from terminals to 25 and 100 mM EtOH are reproduced from a previous publication (Dopico et al., 1996). We did not observe any channels that were inhibited by the drug.

Expression of BK β subunits in the three compartments of the HNS.

JPET Fast Forward. Published on March 25, 2009 as DOI: 10.1124/jpet.108.146175
This article has not been copyedited and formatted. The final version may differ from this version.

One possible explanation for these findings is a selective regional distribution of the auxiliary β1 subunit to the somatic and dendritic compartments, and β4 subunit to the terminal compartment. Iberiotoxin provides a useful pharmacological tool to distinguish αβ4 from α or αβ1 channels. Expression studies have shown that α or αβ1 BK channels are blocked by nanomolar concentrations of the scorpion toxins, iberiotoxin and charybdotoxin, while presence of the β4 subunit renders BK channels insensitive to these toxins (Hanner et al., 1998; Lippiat et al., 2003). To assess iberiotoxin sensitivity, outside-out patches held at +40 mV were perfused with 50 nM iberiotoxin (IbTX) in 5 μM free-Ca^{2+}. IbTX strongly inhibited both dendritic (nPo decreased 81% and 75%, n =2) and somatic channels (nPo decreased 83% and 71%, n = 2) (data not shown). IbTX blockade of somatic channels is consistent with previously reported findings (Dopico et al., 1999). In contrast, IbTX had no effect on BK channels in the terminal (nPo changed 0.5% and 0.2%, n = 2) (data not shown) consistent with previously reported findings that terminal channels are insensitive to blockade by the scorpion toxin, charybdotoxin (Wang et al., 1992). These data support the notion that αβ4 channels are present in the nerve terminal, and absent in both the cell body and dendrite. However, since both α channels and αβ1 channels are iberiotoxin sensitive we were unable to use this pharmacological tool to establish the selective presence of the αβ1 channel in the cell body and dendrite.

To determine whether β1 subunits were present in the somatic and dendritic compartments, we immunolabeled coronal sections of rat SON tissue with antibodies to the β1 or β4 subunit and vasopressin (AVP) neurophysin, a known marker for SON magnocellular neurons (Figure 5). The punctate anti-β1 staining indicates that BK β1 channel clusters are located throughout the cell body, as well as in both proximal and distal dendrites (arrowheads, Figure 5C). In contrast,

surrounding regions of the brain had very low to nonexistent β1 staining, suggesting this antibody is highly specific (Figure 5A). In contrast to the robust β1 staining, β4 staining in SON cell bodies and dendrites was extremely faint (Figure 5B).

To confirm the distribution of β4 subunits to the nerve terminal we immunolabeled dissociated terminals with antibodies to the β1 or β4 subunit, AVP and oxytocin (OXT). We then selected terminals ranging in size from 5-10 μm for image analysis. These terminals, when labeled with the same concentrations used to stain the SON, displayed distinct punctuate β4 clusters (Fig. 6B, left panel) while the β1 subunit was barely detectable (Figure 6A; left panel). Antibody specificity was appropriately controlled for by either omitting the primary antibody or preabsorbing with blocking peptide. Additionally, both the anti-β1 and anti-β4 antibody have been show to be immunoreactive in wild-type mice, with no specific staining in β1- and β4-deficient mice, respectively (Grimm et al., 2007; Piwonska et al., 2008).

We quantified the intensity of the immunofluorescence signal for β1 and β4 antibodies in the dendrites, soma and terminals (Fig. 6C). For β1 subunits, the optical density was much greater in the soma (25.83 ± 2.15; $n = 3$) and the dendrites (27.93 ± 0.07) compared to the terminals (1.97 ± 1.52). Interestingly, the ratio was reversed for β4 expression. Thus, in the soma and dendrites the mean optical density of β4 was 6.75 ± 0.88 and 0.35 ± 0.18, respectively while in the terminals the value was much higher (33.93 ± 3.1).

JPET Fast Forward. Published on March 25, 2009 as DOI: 10.1124/jpet.108.146175
This article has not been copyedited and formatted. The final version may differ from this version.

Discussion

The data presented in this paper demonstrate: (1) the expression of functional BK channels on the membranes of dendrites, somata, and nerve terminals of hypothalamic magnocellular neurons; (2) selective expression of β1 containing BK channels in cell body and dendrite; (3) selective expression of β4 containing BK channels in the nerve terminal; and (4) ethanol potentiation of nerve terminal β4 containing BK channels but not somatic and dendritic β1 containing BK channels.

Regional distribution of BK β subunits in three compartments of a single HNS neuron

This study has examined the characteristics of BK channel subtypes in each of the three compartments of a neuron (dendrite, cell body, and nerve terminal) utilizing the unique advantages of the hypothalamic-neurohypophysial system. In doing so, we discovered that in these neurons, BK channels were similar in the somatic and dendritic compartments. In contrast, we observed markedly different BK channels in the nerve terminal. Properties of both cell body and dendritic BK channels include (1) increased calcium sensitivity compared to nerve terminal channels, manifested as a shift in the voltage required to activate the channel to more hyperpolarized potentials, (2) fast activation kinetics, (3) insensitivity to ethanol and (4) blockade by iberiotoxin. Properties of exogenously expressed αβ1 channels (Jiang et a.,1999; Feinberg-Zadek and Treistman, 2007) match the biophysical and pharmacological properties of HNS somatic and dendritic channels, suggesting the presence of β1 in this compartment.

Nerve terminal channels, on the other hand, display the following properties: (1) decreased calcium sensitivity compared to somatic and dendritic channels, manifested as a shift in the

JPET Fast Forward. Published on March 25, 2009 as DOI: 10.1124/jpet.108.146175
This article has not been copyedited and formatted. The final version may differ from this version.

voltage required to activate the channel to more depolarized potentials, (2) slow activation kinetics, (3) sensitivity to ethanol and (4) insensitivity to iberiotoxin blockade. Consistent with exogenous αβ4 expression studies (Behrens et al., 2000; Feinberg-Zadek and Treistman, 2007), these biophysical and pharmacological properties suggest that HNS nerve terminal channels contain the β4 subunit. Immunostaining with antibodies to either the β1 and β4 subunit confirmed the regional distribution of BK αβ1 channels in the somatic and dendritic compartments and BK αβ4 channels in nerve terminals.

Regional subcellular distribution of channel subtypes is not limited to BK channels, but has also been reported for other channel types. For example, Kv3.1 voltage gated potassium channel splice variants are differentially distributed in the reticular thalamus where the Kv3.1b isoform is localized to the soma and proximal dendrites while the Kv3.1a isoform is selectively restricted to axonal processes (Ozaita et al., 2002). There are also reports that T-type calcium channel isoforms selectively distribute to the soma or dendrite dependent upon neuronal type (McKay et al., 2006). Furthermore, HCN channels display subunit-specific subcellular distribution patterns in the hippocampus dependent upon stage of development (Brewster et al., 2007). These illustrative examples emphasize that the selective distribution of ion channels within a neuron plays an important role in cell polarity and neuronal specialization.

A number of mechanisms may underlie the selective distribution of ion channels within neurons. Several mRNA's such as arginine vasopressin and αCAMKII contain a dendritic localizer sequence (DLS) which targets the mRNA to the dendritic compartment (Mohr and Richter, 2004; Blichenberg et al., 2001). An additional mechanism for controlling localization is through PDZ-

containing anchoring proteins which target G-protein-gated K+ channels (Kir3.2c) to the postsynaptic density in dopaminergic neurons of the substantia nigra (Kurachi and Ishii, 2004). Lastly, β subunits of channels have also been proposed to play a role in localization. For instance, association of the auxiliary β subunit with the calcium channel α1 subunit results in increased membrane localization (Bichet et al., 2000).

Compartment-specific ethanol effects on BK channels are determined by regional specificity of beta subunit

A strong correlation between BK β subunit identity and ethanol sensitivity has been shown in HEK293 expression studies (Feinberg-Zadek and Treistman, 2007) and freshly dissociated rat nucleus accumbens neurons (Martin et al., 2004). In medium spiny neurons the effects of EtOH on BK channels are regionally specific, similar to the HNS. Interestingly, in contrast to the HNS, BK channels in the cell bodies of medium spiny neurons are sensitive to EtOH, while those in dendrites are insensitive to the drug. In these neurons, this dichotomy correlates with the differential distribution of β1 and β4 subunit to the dendrite and soma, respectively. Likewise, we suggest that the observed differences in ethanol sensitivity between HNS somatic, dendritic and nerve terminal channels reflect a differential distribution of β1 and β4 subunits.

A link between subunit composition and ethanol sensitivity has also been reported for other ion channels. For example, the effects of ethanol on P2X receptors are dependent upon receptor subtype, with P2X3 receptors potentiated and P2X4 receptors inhibited by EtOH (Davies et al., 2005). NMDA receptor NR2 subunits and NR1 splice variants are also thought to confer

differential sensitivity to EtOH-induced inhibition of NMDA currents (Chu et al., 1995). Furthermore, various AMPA receptor subtypes are also differentially sensitive to ethanol (Akinshola et al., 2003).

While we propose that regional ethanol sensitivity within magnocellular neurons in the HNS is conferred through subunit composition several other factors may also play a role. These factors include variations in BK α subunit splice variants, regional differences in lipid bilayer composition, and posttranslational modification. For example, expression studies in HEK293 cells indicate that certain BK α isoforms such as STREX are alcohol insensitive (Pietrzykowski et al., 2008). In addition, bilayer studies have shown that modulation of the lipid environment can alter BK channel sensitivity to ethanol (Crowley et al., 2005). Lastly, posttranslational modifications including phosphorylation status of BK channels have also been shown to alter ethanol sensitivity (Liu et al., 2006).

Functional implications

The selective regional distribution of alcohol sensitive and insensitive channels in the HNS has interesting implications for synaptic integration. The SON receives excitatory glutamatergic inputs from areas such as the amygdala, the suprachiasmatic nucleus, and the lamina terminalis (Csaki et al., 2002). In addition, the SON receives inhibitory GABAergic inputs from areas such as the nucleus accumbens, a region known to play a role in addiction (Shibuki, 1984). Both excitatory glutamatergic and inhibitory GABAergic inputs establish synaptic contact primarily on the dendrites of the SON, which generally comprise approximately 80% of the neuron's surface area. The selective distribution of dendritic channels insensitive to acute EtOH may suggest that

JPET Fast Forward. Published on March 25, 2009 as DOI: 10.1124/jpet.108.146175
This article has not been copyedited and formatted. The final version may differ from this version.

the effects of alcohol on HNS neurons mediated through BK channels have little direct impact on the integration of dendritic electrical activity. Instead, the selective distribution of ethanol sensitive BK channels to the nerve terminal compartment suggests that the effect of alcohol on HNS neurons mediated through BK channels is largely confined to the nerve terminal.

In addition to the role that nerve terminal BK channels play in mediating HNS responses to ethanol, somatic and dendritic BK channels may also indirectly contribute to ethanol effects, despite their apparent insensitivity to the drug. This possibility exists because BK channels can form heteromultimeric complexes with both voltage-gated calcium channels and NMDA receptors (Marrion and Tavalin, 1998; Isaacson and Murphy, 2001). Ethanol inhibits voltage-gated calcium channels and NMDA receptors thereby lowering intracellular calcium levels (Widmer et al., 1998). As a result, ethanol induced changes in intracellular dendritic calcium levels may be transduced by associated calcium-activated BK channels, ultimately influencing input and output patterns of HNS neurons. Thus, the presence of BK channels in somatic, dendritic and nerve terminal compartments of HNS neurons, and their corresponding differential sensitivity to ethanol, may play an important role in the response to ethanol.

Peptide hormone release

In the HNS, all three cellular compartments (dendrite, soma and nerve terminal) secrete the peptides oxytocin (OXT) and vasopressin (AVP). The dendrites and cell bodies of magnocellular neurons release OXT and AVP centrally into the brain, while nerve terminals release OXT and AVP peripherally into systemic circulation. It is of particular interest that while both dendrites and nerve terminals secrete AVP and OXT, release from these two compartments can occur independently and is differently regulated (reviewed in Ludwig and

JPET Fast Forward. Published on March 25, 2009 as DOI: 10.1124/jpet.108.146175
This article has not been copyedited and formatted. The final version may differ from this version.

Leng, 2006). In terminals, peptide release is regulated in an activity dependent manner when membrane depolarization elicits calcium entry through voltage-gated calcium channels. Dendritic release, on the other hand, is triggered not only by depolarization induced calcium entry, but also by the release of calcium from intracellular stores in response to the binding of AVP or OXT to its corresponding autoreceptor. Our study shows that these two compartments, the nerve terminal and dendrite, have distinctly different BK channels with varying calcium sensitivities, which may contribute to differences in the regulation of peptide release.

Acknowledgements

We thank Andy Wilson, Sonia Ortiz-Miranda, and José Lemos for their technical and critical advice.

JPET Fast Forward. Published on March 25, 2009 as DOI: 10.1124/jpet.108.146175
This article has not been copyedited and formatted. The final version may differ from this version.

References

Akinshola BE, Yasuda RP, Peoples RW, and Taylor RE (2003) Ethanol sensitivity of recombinant homomeric and heteromeric AMPA receptor subunits expressed in Xenopus oocytes. *Alcohol Clin.Exp.Res.* **27**:1876-1883.

Behrens R, Nolting A, Reimann F, Schwarz M, Waldschutz R, and Pongs O (2000) hKCNMB3 and hKCNMB4, cloning and characterization of two members of the large-conductance calcium-activated potassium channel beta subunit family. *FEBS Lett.* **474**:99-106.

Benhassine N and Berger T (2005) Homogeneous distribution of large-conductance calcium-dependent potassium channels on soma and apical dendrite of rat neocortical layer 5 pyramidal neurons. *Eur.J.Neurosci.* **21**:914-926.

Bichet D, Cornet V, Geib S, Carlier E, Volsen S, Hoshi T, Mori Y, and De Waard M (2000) The I-II loop of the Ca2+ channel alpha1 subunit contains an endoplasmic reticulum retention signal antagonized by the beta subunit. *Neuron* **25**:177-190.

Blichenberg A, Rehbein M, Muller R, Garner CC, Richter D, and Kindler S (2001) Identification of a cis-acting dendritic targeting element in the mRNA encoding the alpha subunit of Ca2+/calmodulin-dependent protein kinase II. *Eur.J.Neurosci.* **13**:1881-1888.

Brenner R, Jegla TJ, Wickenden A, Liu Y, and Aldrich RW (2000) Cloning and functional characterization of novel large conductance calcium-activated potassium channel beta subunits, hKCNMB3 and hKCNMB4. *J.Biol.Chem.* **275**:6453-6461.

Brewster AL, Chen Y, Bender RA, Yeh A, Shigemoto R, and Baram TZ (2007) Quantitative analysis and subcellular distribution of mRNA and protein expression of the

hyperpolarization-activated cyclic nucleotide-gated channels throughout development in rat hippocampus. *Cereb.Cortex* **17**:702-712.

Chu B, Anantharam V, and Treistman SN (1995) Ethanol inhibition of recombinant heteromeric NMDA channels in the presence and absence of modulators. *J.Neurochem.* **65**:140-148.

Crowley JJ, Treistman SN, and Dopico AM (2005) Distinct structural features of phospholipids differentially determine ethanol sensitivity and basal function of BK channels. *Mol.Pharmacol.* **68**:4-10.

Csaki A, Kocsis K, Kiss J, and Halasz B (2002) Localization of putative glutamatergic/aspartatergic neurons projecting to the supraoptic nucleus area of the rat hypothalamus. *Eur.J.Neurosci.* **16**:55-68.

Davies DL, Kochegarov AA, Kuo ST, Kulkarni AA, Woodward JJ, King BF, and Alkana RL (2005) Ethanol differentially affects ATP-gated P2X(3) and P2X(4) receptor subtypes expressed in Xenopus oocytes. *Neuropharmacology* **49**:243-253.

Dopico AM, Lemos JR, and Treistman SN (1996) Ethanol increases the activity of large conductance, Ca(2+)-activated K+ channels in isolated neurohypophysial terminals. *Mol.Pharmacol.* **49**:40-48.

Dopico AM, Widmer H, Wang G, Lemos JR, and Treistman SN (1999) Rat supraoptic magnocellular neurones show distinct large conductance, Ca2+-activated K+ channel subtypes in cell bodies versus nerve endings. *J.Physiol* **519 Pt 1**:101-114.

Dworetzky SI, Boissard CG, Lum-Ragan JT, McKay MC, Post-Munson DJ, Trojnacki JT, Chang CP, and Gribkoff VK (1996) Phenotypic alteration of a human BK (hSlo) channel by hSlobeta subunit coexpression: changes in blocker sensitivity, activation/relaxation and inactivation kinetics, and protein kinase A modulation. *J.Neurosci.* **16**:4543-4550.

Feinberg-Zadek PL and Treistman SN (2007) Beta-subunits are important modulators of the acute response to alcohol in human BK channels. *Alcohol Clin.Exp.Res.* **31**:737-744.

Grimm PR, Foutz RM, Brenner R, and Sansom SC (2007) Identification and localization of BK-beta subunits in the distal nephron of the mouse kidney. *Am.J.Physiol Renal Physiol* **293**:F350-F359.

Hanner M, Vianna-Jorge R, Kamassah A, Schmalhofer WA, Knaus HG, Kaczorowski GJ, and Garcia ML (1998) The beta subunit of the high conductance calcium-activated potassium channel. Identification of residues involved in charybdotoxin binding. *J.Biol.Chem.* **273**:16289-16296.

Isaacson JS and Murphy GJ (2001) Glutamate-mediated extrasynaptic inhibition: direct coupling of NMDA receptors to Ca(2+)-activated K+ channels. *Neuron* **31**:1027-1034.

Jiang Z, Wallner M, Meera P, and Toro L (1999) Human and rodent MaxiK channel beta-subunit genes: cloning and characterization. *Genomics* **55**:57-67.

Knaus HG, Garcia-Calvo M, Kaczorowski GJ, and Garcia ML (1994) Subunit composition of the high conductance calcium-activated potassium channel from smooth muscle, a representative of the mSlo and slowpoke family of potassium channels. *J.Biol.Chem.* **269**:3921-3924.

Kurachi Y and Ishii M (2004) Cell signal control of the G protein-gated potassium channel and its subcellular localization. *J.Physiol* **554**:285-294.

Lippiat JD, Standen NB, Harrow ID, Phillips SC, and Davies NW (2003) Properties of BK(Ca) channels formed by bicistronic expression of hSloalpha and beta1-4 subunits in HEK293 cells. *J.Membr.Biol.* **192**:141-148.

Liu J, Asuncion-Chin M, Liu P, and Dopico AM (2006) CaM kinase II phosphorylation of slo Thr107 regulates activity and ethanol responses of BK channels. *Nat.Neurosci.* **9**:41-49.

Ludwig M and Leng G (2006) Dendritic peptide release and peptide-dependent behaviours. *Nat.Rev.Neurosci.* **7**:126-136.

Madeira MD, Sousa N, Lieberman AR, and Paula-Barbosa MM (1993) Effects of chronic alcohol consumption and of dehydration on the supraoptic nucleus of adult male and female rats. *Neuroscience* **56**:657-672.

Marrion NV and Tavalin SJ (1998) Selective activation of Ca2+-activated K+ channels by co-localized Ca2+ channels in hippocampal neurons. *Nature* **395**:900-905.

Martin G, Puig S, Pietrzykowski A, Zadek P, Emery P, and Treistman S (2004) Somatic localization of a specific large-conductance calcium-activated potassium channel subtype controls compartmentalized ethanol sensitivity in the nucleus accumbens. *J.Neurosci.* **24**:6563-6572.

McKay BE, McRory JE, Molineux ML, Hamid J, Snutch TP, Zamponi GW, and Turner RW (2006) Ca(V)3 T-type calcium channel isoforms differentially distribute to somatic and dendritic compartments in rat central neurons. *Eur.J.Neurosci.* **24**:2581-2594.

McManus OB (1991) Calcium-activated potassium channels: regulation by calcium. *J.Bioenerg.Biomembr.* **23**:537-560.

Mohr E and Richter D (2004) Subcellular vasopressin mRNA trafficking and local translation in dendrites. *J.Neuroendocrinol.* **16**:333-339.

Ozaita A, Martone ME, Ellisman MH, and Rudy B (2002) Differential subcellular localization of the two alternatively spliced isoforms of the Kv3.1 potassium channel subunit in brain. *J.Neurophysiol.* **88**:394-408.

Pietrzykowski AZ, Friesen RM, Martin GE, Puig SI, Nowak CL, Wynne PM, Siegelmann HT, and Treistman SN (2008) Posttranscriptional regulation of BK channel splice variant stability by miR-9 underlies neuroadaptation to alcohol. *Neuron* **59**:274-287.

Pietrzykowski AZ, Martin GE, Puig SI, Knott TK, Lemos JR, and Treistman SN (2004) Alcohol tolerance in large-conductance, calcium-activated potassium channels of CNS terminals is intrinsic and includes two components: decreased ethanol potentiation and decreased channel density. *J.Neurosci.* **24**:8322-8332.

Piwonska M, Wilczek E, Szewczyk A, and Wilczynski GM (2008) Differential distribution of Ca(2+)-activated potassium channel beta4 subunit in rat brain: Immunolocalization in neuronal mitochondria. *Neuroscience* **153**:446-460.

Ruela C, Sousa N, Madeira MD, and Paula-Barbosa MM (1994) Stereological study of the ultrastructural changes induced by chronic alcohol consumption and dehydration in the supraoptic nucleus of the rat hypothalamus. *J.Neurocytol.* **23**:410-421.

Sailer CA, Kaufmann WA, Kogler M, Chen L, Sausbier U, Ottersen OP, Ruth P, Shipston MJ, and Knaus HG (2006) Immunolocalization of BK channels in hippocampal pyramidal neurons. *Eur.J.Neurosci.* **24**:442-454.

Shibuki K (1984) Supraoptic neurosecretory cells: synaptic inputs from the nucleus accumbens in the rat. *Exp.Brain Res.* **53**:341-348.

Wallner M, Meera P, and Toro L (1996) Determinant for beta-subunit regulation in high-conductance voltage-activated and Ca(2+)-sensitive K+ channels: an additional transmembrane region at the N terminus. *Proc.Natl.Acad.Sci.U.S.A* **93**:14922-14927.

Wang G, Thorn P, and Lemos JR (1992) A novel large-conductance Ca(2+)-activated potassium channel and current in nerve terminals of the rat neurohypophysis. *J.Physiol* **457**:47-74.

Widmer H, Lemos JR, and Treistman SN (1998) Ethanol reduces the duration of single evoked spikes by a selective inhibition of voltage-gated calcium currents in acutely dissociated supraoptic neurons of the rat. *J.Neuroendocrinol.* **10**:399-406.

Footnotes

These studies were supported by the National Institute on Alcohol Abuse and Alcoholism of the National Institutes of Health [Grants 1 F31 AA015474-01A1, 5 RO1 AA 08003-18, and R37 AA12054-03].

JPET Fast Forward. Published on March 25, 2009 as DOI: 10.1124/jpet.108.146175
This article has not been copyedited and formatted. The final version may differ from this version.

Legends for Figures

Figure 1. Voltage and calcium dependence of dendritic BK channels of HNS magnocellular neurons. (A) Micrograph of a recording electrode positioned on the dendrite of a dissociated SON neuron. (B) The time spent in the open state by two dendritic BK channels, recorded in inside-out patch clamp configuration in the presence of 5 μM free-Ca^{2+}, increases as the membrane is depolarized. (C) Traces recorded at -40 mV in the same patch as in *B* show the dependence of channel activity on intracellular calcium (1-10 μM). (D) Plot of BK channel current amplitude as a function of membrane potential calculated from results in panel B. A linear fit of this relationship (r = 0.99) gave a BK channel unitary conductance of 261 pS. C and O represent the closed and open states, respectively. The number next to the letter O represents the number of channel(s) simultaneously open.

Figure 2. Comparison of the conductance and calcium dependence of somatic, dendritic, and nerve terminal BK channels. (A) Mean conductance of somatic, dendritic, and nerve terminal channels measured in the presence of 5 and 10 μM free-Ca^{2+}. (B) Normalized NPo-Voltage relationship of SON somatic and dendritic channels compared to SON nerve terminal channels in 10 μM free-Ca^{2+} (SEM not shown to reduce clutter). Somatic, dendritic, and nerve terminal are shown as triangles, squares, and circles, respectively. (C) Plots of normalized mean NPo as a function of voltage at different [Ca^{2+}]i; circles, 5 μM; squares, 10 μM; triangles, 25 μM. Open and filled symbols represent soma and dendrite, respectively. The NPo-V relationship, fitted with a Boltzmann equation, is shifted along the voltage axis to more negative potentials as $[Ca^{2+}]_i$ increases.

Figure 3. Gating properties of nerve terminal channels differ from that of somatic and dendritic channels. A series of seven consecutive BK traces evoked by depolarizing (A) somatic, (B) dendritic, or (C) nerve terminal membrane patches from 0 to +40 mV. Channel activity was recorded in 10 μM free-Ca^{2+} in an inside-out patch. C and O1 represent the closed and open states, respectively. D, E and F represent the aggregate of 100 consecutive individual single channel traces recorded from one BK channel in a membrane patch excised from soma, dendrite and terminal compartments, respectively. In all cases, BK current activation was best fit with a single exponential whose value (τ) is indicated below the aggregate traces.

Figure 4. Ethanol (EtOH) exposure increases BK channel activity in the nerve terminal but not in soma or dendrite. Traces of BK channel activity before and during exposure to 50 mM EtOH (V_h = -40 mV, 5 μM free-Ca^{2+}) in (A) dendrite, (B) soma, or (C) nerve terminal patches. C and O1 represent the closed and open state, respectively. (D) Plot of the effects of various EtOH concentrations on somatic, dendritic, and terminal BK channels. The numbers within the bars represent the number of patches tested. The asterisk indicates statistical significance of $p < 0.01$. Data showing the response to 25 and 100 mM EtOH of BK channels in terminals are from a previous publication (Dopico et al., 1996).

Figure 5. Punctate clusters of BK β1 subunits are located in the cell body and peripheral processes of magnocellular neurons. 20X magnification of a section from fixed adult rat brain immunolabeled with (A) anti-β4 followed by mouse secondary Alexa 488 conjugated antibody or (B) anti-β1 and Alexa 488 conjugated antibody. (C) 63X magnification of two neurons labeled with anti-β1 and Alexa 488 conjugated antibody. The sections in panels *A-C* are counterstained

with anti-vasopressin (AVP) neurophysin and Alexa 594 conjugated antibody. Arrowheads indicate stained dendrites.

Figure 6. BK β4 subunits in HNS nerve terminals. Single HNS nerve terminals magnified at 63X immunolabeled with (A) anti-β1 and mouse secondary Alexa 594 conjugated antibody or (B) anti-β4 and mouse secondary Alexa 594 conjugated antibody. Nerve terminals are counterstained with (1) anti-vasopressin (AVP) neurophysin and rabbit secondary Alexa 350 conjugated antibody and (2) anti-oxytocin (OXT) and rabbit secondary Alexa 488 conjugated antibody. (C) Pie charts of the optical density of β1 (left chart) and β4 (right chart) immuno-fluorescence in the dendrite (red), soma (blue) and terminal (yellow) compartments of SON neurons.

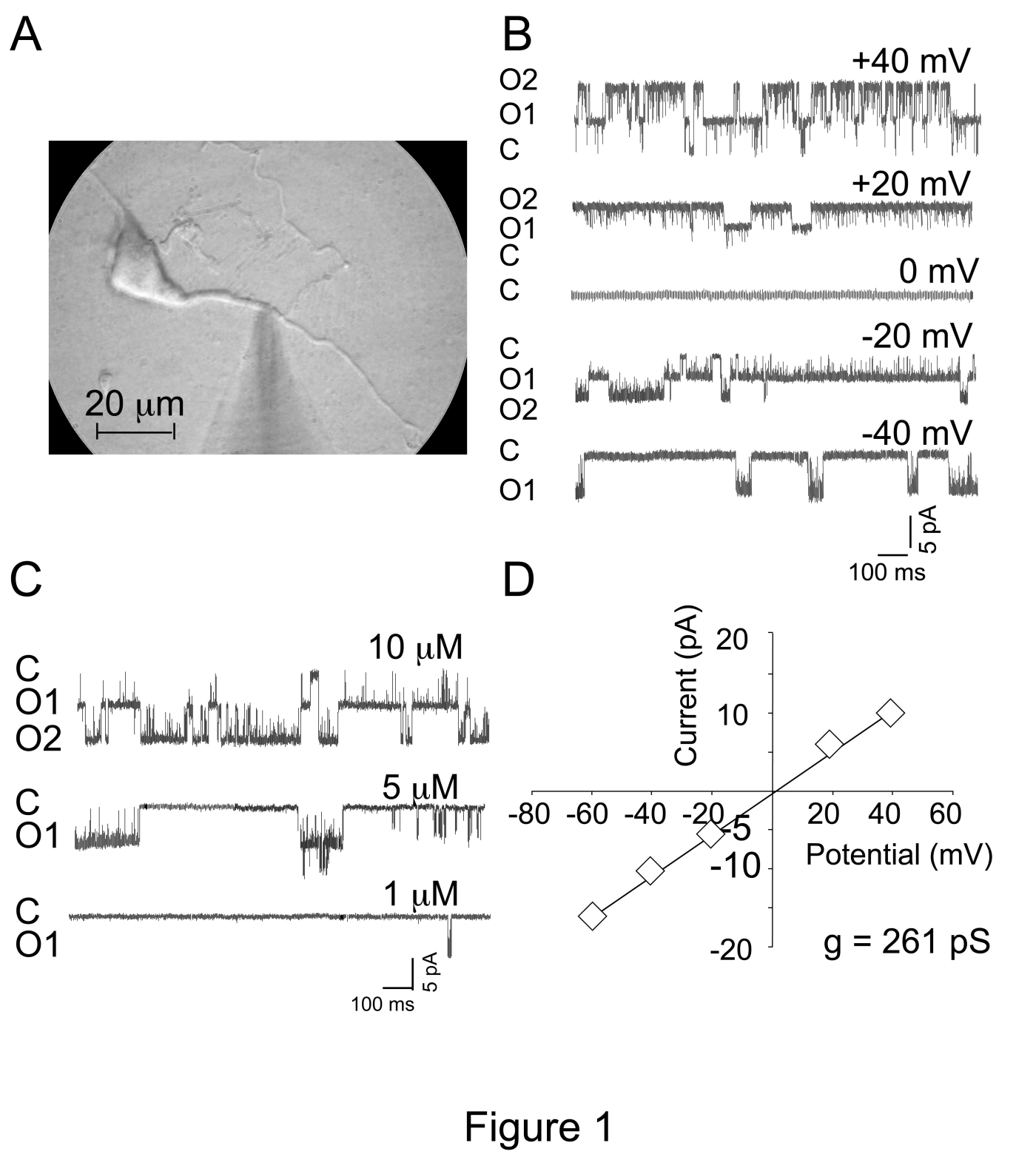
A
20 μm
B
+40 mV
O2
O1
C
+20 mV
O2
O1
C
0 mV
C
C
-20 mV
O1
O2
C
-40 mV
O1
5 pA
100 ms
C
10 μM
C
O1
O2
5 μM
C
O1
1 μM
C
O1
5 pA
100 ms
D
Current (pA)
20
10
-5
-10
-20
-80 -60 -40 -20
20 40 60
Potential (mV)
g = 261 pS

Figure 1

JPET Fast Forward. Published on March 25, 2009 as DOI: 10.1124/jpet.108.146175
This article has not been copyedited and formatted. The final version may differ from this version.

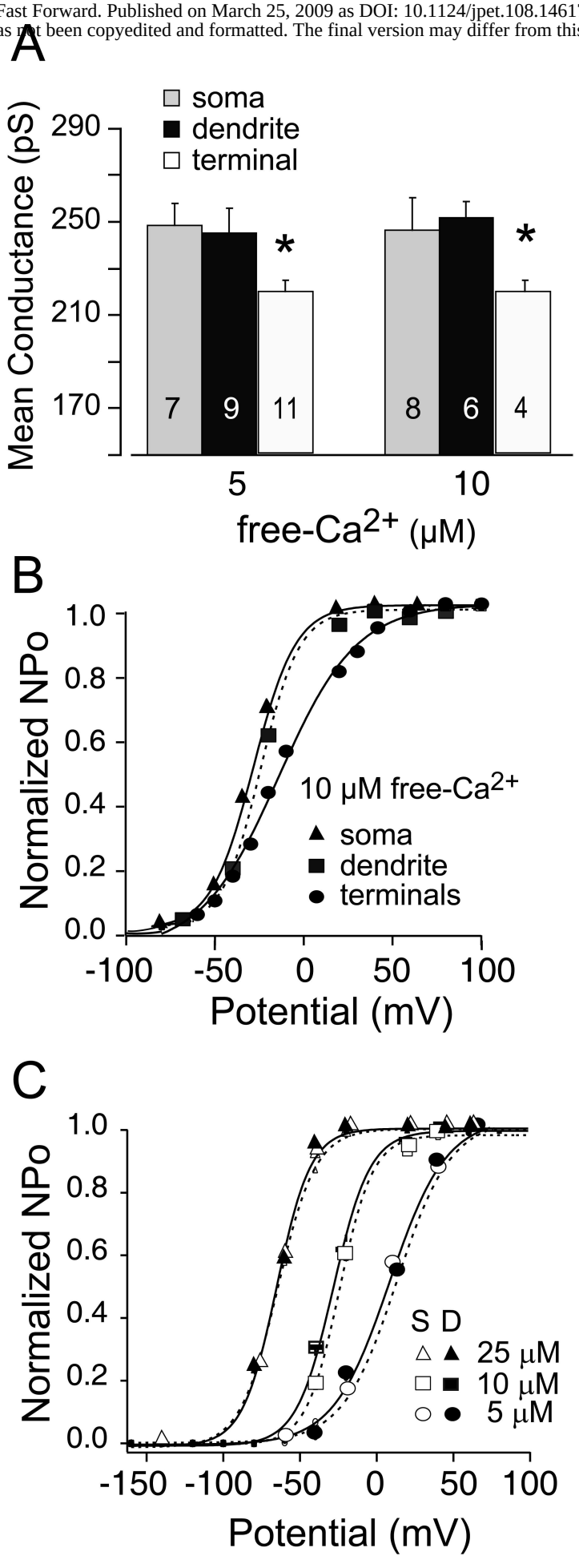

Figure 2

JPET Fast Forward. Published on March 25, 2009 as DOI: 10.1124/jpet.108.146175
This article has not been copyedited and formatted. The final version may differ from this version.

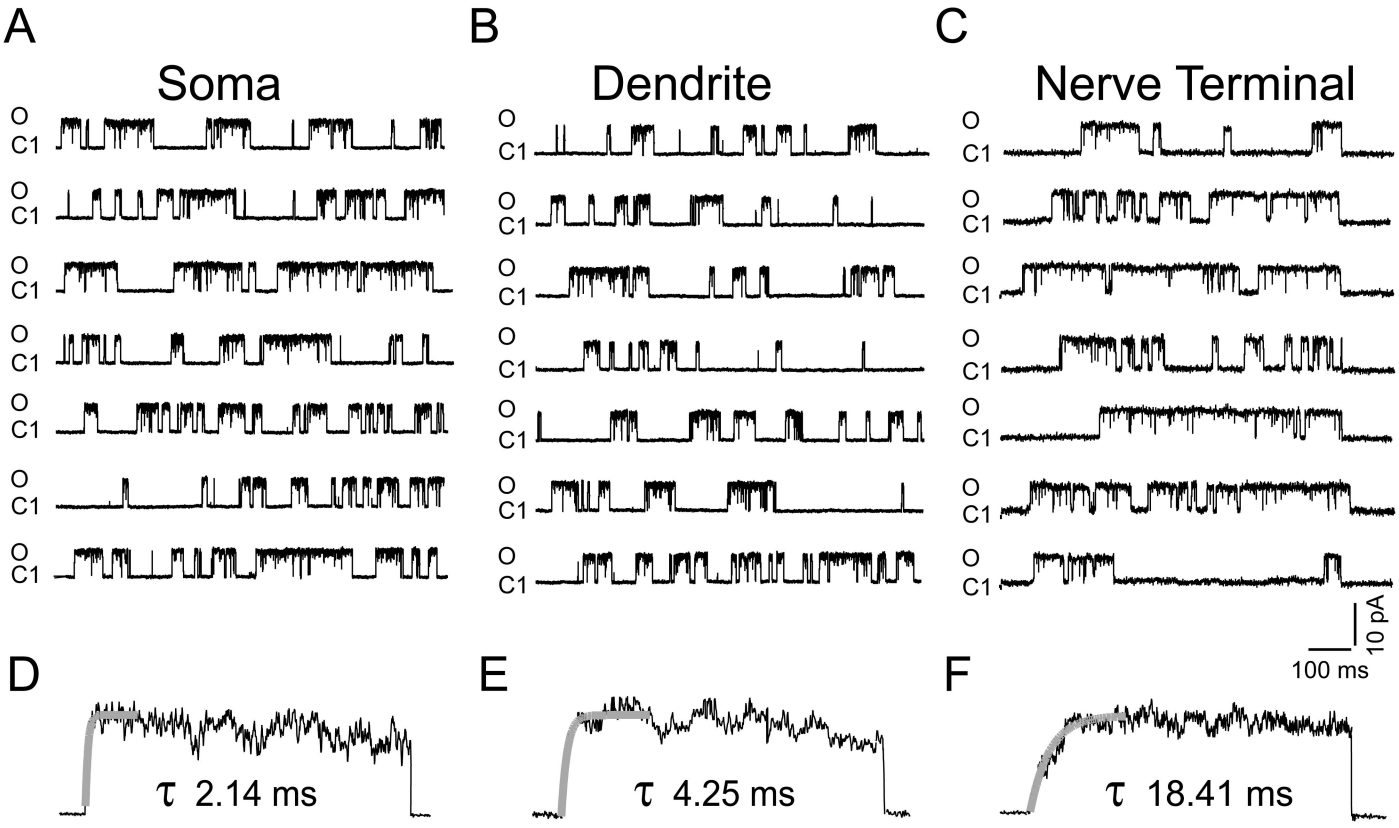

Figure 3

JPET Fast Forward. Published on March 25, 2009 as DOI: 10.1124/jpet.108.146175
This article has not been copyedited and formatted. The final version may differ from this version.

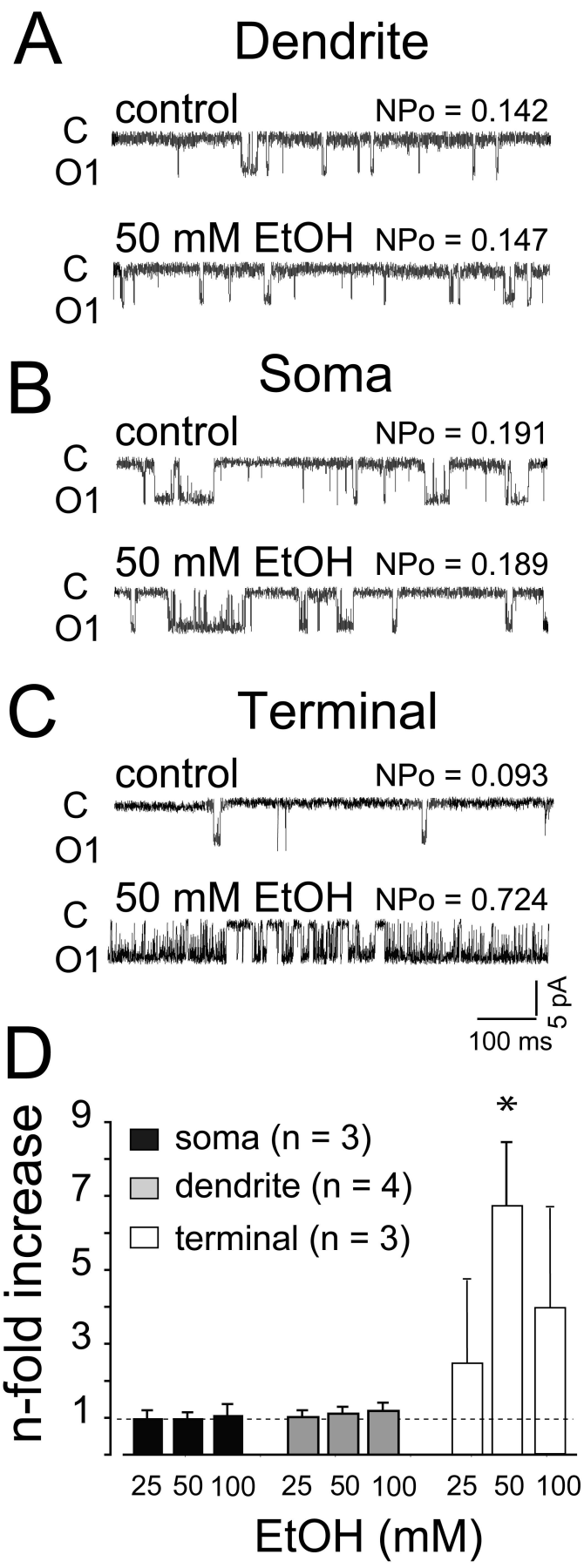

Figure 4

JPET Fast Forward. Published on March 25, 2009 as DOI: 10.1124/jpet.108.146175
This article has not been copyedited and formatted. The final version may differ from this version.

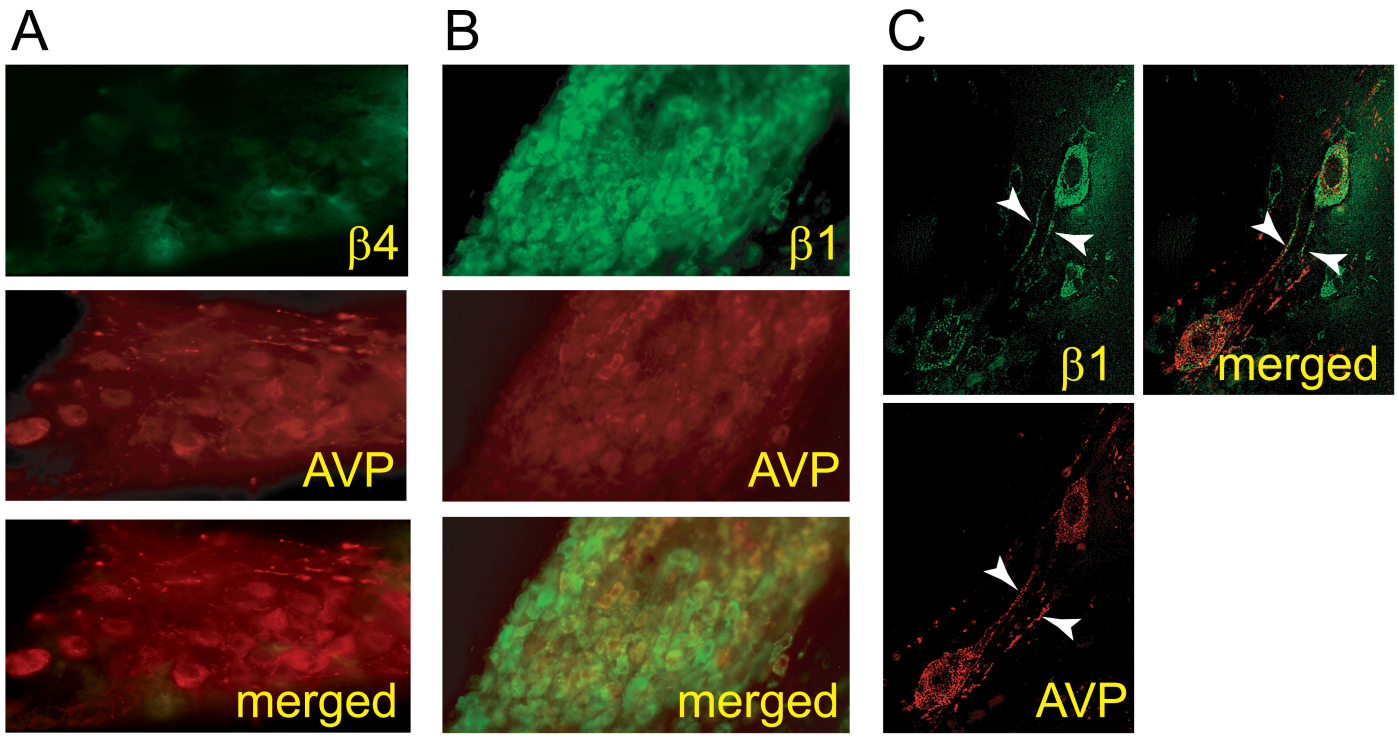

Figure 5

JPET Fast Forward. Published on March 25, 2009 as DOI: 10.1124/jpet.108.146175
This article has not been copyedited and formatted. The final version may differ from this version.

Figure 6